Structural Durability & Health Monitoring

Tech Science Press

Doi:10.32604/sdhm.2025.061805

ARTICLE

A Combined Denoising Method of Adaptive VMD and Wavelet Threshold for Gear Health Monitoring

Guangfei Jia*, Jinqiu Yang and Hanwen Liang

School of Mechanical Engineering, Hebei University of Science and Technology, Shijiazhuang, 050018, China

*Corresponding Author: Guangfei Jia. Email: jiagf_11@163.com

Received: 03 December 2024; Accepted: 13 February 2025; Published: 30 June 2025

ABSTRACT: Considering the noise problem of the acquisition signals from mechanical transmission systems, a novel denoising method is proposed that combines Variational Mode Decomposition (VMD) with wavelet thresholding. The key innovation of this method lies in the optimization of VMD parameters K and α using the improved Horned Lizard Optimization Algorithm (IHLOA). An inertia weight parameter is introduced into the random walk strategy of HLOA, and the related formula is improved. The acquisition signal can be adaptively decomposed into some Intrinsic Mode Functions (IMFs), and the high-noise IMFs are identified based on a correlation coefficient-variance method. Further noise reduction is achieved using wavelet thresholding. The proposed method is validated using simulated signals and experimental signals, and simulation results indicate that the proposed method surpasses original VMD, Empirical Mode Decomposition (EMD), and wavelet thresholding in terms of Signal-to-Noise Ratio (SNR) and Root Mean Square Error (RMSE), and experimental results indicate that the proposed method can effectively remove noise in terms of three evaluation metrics. Furthermore, compared with Feature Mode Decomposition (FMD) and Multichannel Singular Spectrum Analysis (MSSA), this method has a better envelope spectrum. This method not only provides a solution for noise reduction in signal processing but also holds significant potential for applications in structural health monitoring and fault diagnosis.

KEYWORDS: Improve horned lizard optimization algorithm; variational mode decomposition; wavelet threshold; inertial weight; secondary noise reduction; structural health monitoring

1 Introduction

In the diagnosis of mechanical system faults, vibration monitoring is a commonly used technique [1,2]. However, the complicated vibration signals generated by equipment during prolonged operation are often contaminated by noise interference, which may come from sources such as the external environment, sensor errors, and other factors. These noises can obscure critical information in the signals, thereby compromising the accuracy of fault diagnosis. To enhance diagnostic accuracy, researchers have proposed various denoising methods [3,4], among which signal decomposition techniques, such as EMD [5,6] and VMD [7,8], are widely applied. Currently, research on health monitoring and fault diagnosis of mechanical systems focuses on improving signal processing and feature extraction methods. Toffghi Niaki et al. [9] proposed a novel approach for early gearbox fault monitoring by combining VMD (Variational Mode Decomposition) and TSA (Time Synchronous Averaging) techniques. Matania et al. [10] introduced a cross-machine health monitoring method to address data scarcity issues and target domain adaptation. Wang et al. [11] analyzed vibration signals using the AR (Auto-Regressive) model to capture gear fault feature patterns. These studies

have advanced the development of mechanical fault diagnosis technology, achieving significant progress particularly in signal processing and cross-domain applications. Wang et al. [12] developed gear signal decomposition techniques, providing new methods for analyzing complex vibration signals. The aforementioned methods have made substantial progress in the application of signal processing. Nevertheless, traditional noise reduction methods often struggle to handle complicated vibration signals, necessitating the development of more advanced techniques.

The EMD method has inherent advantages in analyzing non-stationary and nonlinear signals [13], and it can also be used for signal denoising. However, EMD is prone to problems such as mode aliasing and the endpoint effects. With the progress of research, the EEMD method [14,15] was introduced, which adds white noise to mitigate these issues. Nonetheless, the white noise in EEMD cannot entirely eliminate the problems. The CEEMD method [16] was proposed to further reduce the impact of white noise. Even with these improvements, CEEMD still encounters residual noise in the signal reconstruction process. To solve this problem, the CEEMDAN method [17] was proposed, incorporating adaptive noise to optimize the decomposition process. Nevertheless, EMD and its derivatives continue to face challenges such as mode aliasing and residual noise in the analysis of complex signals.

Based on wavelet analysis, Gilles proposed the Empirical Wavelet Transform (EWT) [18], which is achieved by segmenting the Fourier frequency. However, this segmentation can result in the splitting of characteristic signals into different modes [19]. To solve these problems, VMD [20,21] was introduced, which utilized classical Wiener filtering, Hilbert transform, and frequency mixing for adaptive signal decomposition. Then, the decomposition results can be denoised through filtering or reconstruction. Usually, the parameters K and α of VMD are set based on experience, which may affect both the decomposition and denoising performance [22]. To address this issue, researchers have explored the use of optimization algorithms to automatically select these parameters. For instance, Lin et al. [23] utilized optimized VMD parameters with a CS-improved algorithm and combined them with probabilistic neural networks for gearbox fault diagnosis. Zhang et al. [24] applied the GMPSO-VMD algorithm for fault diagnosis of vibration signal. Ding et al. [25] proposed a Genetic Mutation Particle Swarm Optimization algorithm to optimize VMD parameters, identifying optimal parameter combinations for accurate bearing fault feature extraction.

Due to the ability of VMD to preserve functional signal components for reconstruction, it effectively removes the noise in the original signal. However, some details may be lost during this process. To further improve the decomposition quality of vibration signals, this paper proposes the use of wavelet thresholding for secondary denoising of IMFs that contain high noise level after adaptive VMD decomposition. Specifically, wavelet thresholding is applied to process these high-noise IMFs, effectively suppressing the noise while preserving the main features of the signal. This secondary denoising allows for more accurate extraction of meaningful information from the signal, enhancing the overall effectiveness of vibration signal processing.

2 IHLOA-VMD-Wavelet Thresholding Combined Denoising Method

The combined denoising method consists of two steps. The first step involves decomposing the original vibration signal using VMD. The second step applies wavelet thresholding to denoise the high-noise components. Finally, the original signal with reduced noise content is reconstructed by combining the secondary denoised components, resulting in a new signal.

VMD improves signal denoising by imposing constraints on the center frequency and bandwidth of each mode. Additionally, VMD demonstrates high computational efficiency when processing large-scale datasets. However, the modal number K and penalty parameter α in VMD must be manually set, which complicates the achievement of optimal results in practical applications. This paper employs the HLOA to optimize the two parameters to address this issue. The HLOA was proposed by Peraza-Vázquez et al. [26]

simulating the defense behavior of horned lizards. Compared to other optimization algorithms, HLOA offers faster convergence and enhanced global search capabilities. Since VMD does not fully eliminate noise during the denoising process, wavelet thresholding is applied for secondary denoising of high-noise components after VMD decomposition.

The main steps of the combined denoising method are shown in Fig. 1:

(1) Input the vibration signal, set the HLOA population size to 30, and the number of iterations to 10. Use envelope entropy as the fitness function.

(2) Set the range of the number of decomposition modes K to $[2, 10]$, and the range of the penalty parameter α to $[10, 5000]$.

(3) Input the positions of the horned lizards into VMD to obtain the local minimum of the envelope entropy for the decomposed IMF components.

(4) Compare the envelope entropy values and update the horned lizard positions accordingly.

(5) Check if the stopping condition is met. If not, continue the optimization process and output the optimal parameter combination.

(6) The IHLOA algorithm optimizes the VMD, which then decomposes the signal into K IMFs.

(7) Screen high- and low-noise components based on the correlation coefficient-variance.

(8) After reconstructing the high-noise components, apply wavelet thresholding for secondary denoising, and combine the processed high-noise components with the low-noise components to obtain a combined denoised signal.

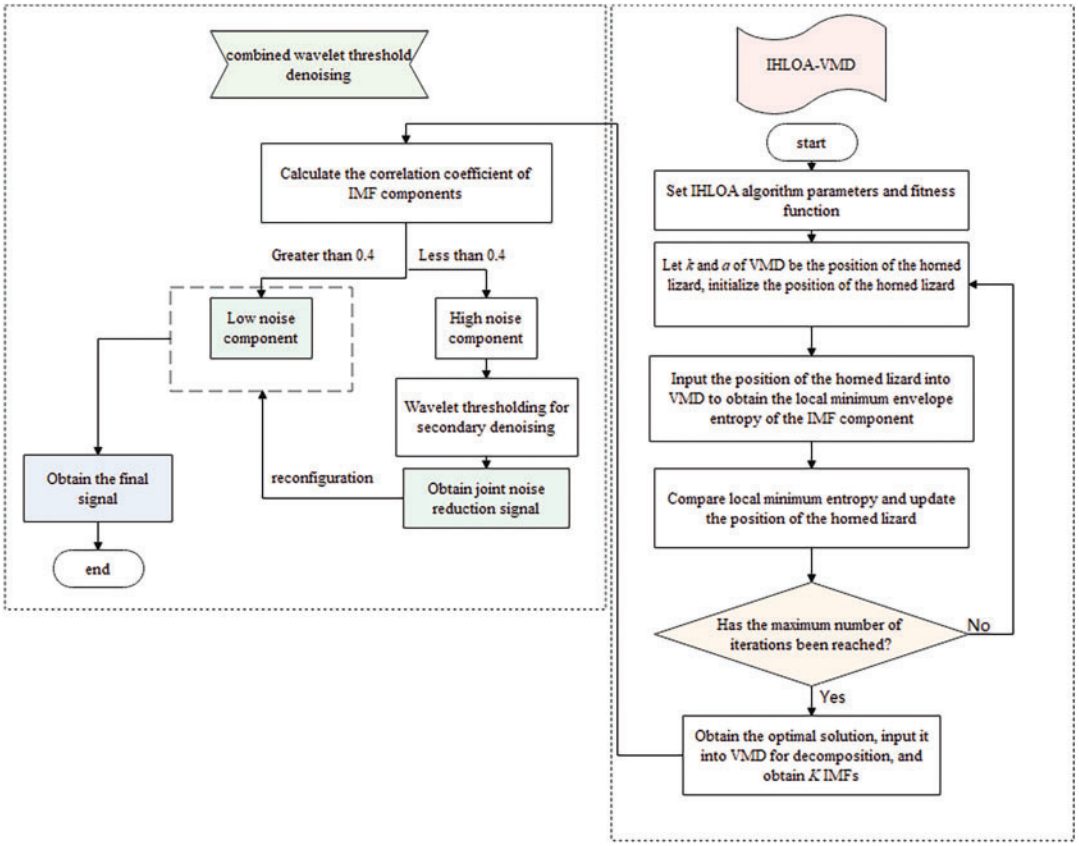

Figure 1: IHLOA-VMD wavelet threshold joint denoising method

3 The Improved Horned Lizard Optimization Algorithm

3.1 Theoretical Basis for Improved Horned Lizard Optimization Algorithm

However, in the HLOA, as the number of iterations increases, the algorithm's convergence speed accelerates, but it struggles to escape from local optimal solutions. To address this issue, the HLOA is improved by introducing an inertia weight parameter ω into the random fast movement strategy.

The inertia weight parameter ω plays a crucial role: a larger ω enhances the algorithm's global search capability, allowing it to quickly traverse the search space and find better solutions, while a smaller ω helps refine the search, enabling the algorithm to explore more thoroughly around the discovered optimal solutions and further improve the solution quality. The formula for ω is as follows:

$$\omega = cos\left(\frac{\pi}{2} \times \left(1 - \frac{t}{T_{max}}\right)\right) \tag{1}$$

In the equation: t—The current iteration number.

Original Position Update Formula:

$$\vec{x}_i\,(t+1) = \vec{x}_{best}\,(t) + walk\left(\frac{1}{2} - \varepsilon\right)\vec{x}_i\,(t) \tag{2}$$

Improved Position Update Formula:

$$X(\mathrm{t}+1) = \omega \cdot X\,(t) + + walk\left(\frac{1}{2} - \varepsilon\right) \cdot \left(\vec{x}_{best}\,(t) - \vec{x}_i\,(t)\right) \tag{3}$$

3.2 Performance Evaluation of Improved Algorithm

The performance of the IHLOA is validated using essential standard test functions, as shown in Fig. 2. It can be observed that the convergence speed of the IHLOA is faster than that of other algorithms. Its fitness value decreases exponentially, indicating a strong global search capability. The IHLOA can quickly escape local optima and demonstrates good local search ability. The improved HLOA enhances both global and local search capabilities, resulting in better convergence speed and search accuracy.

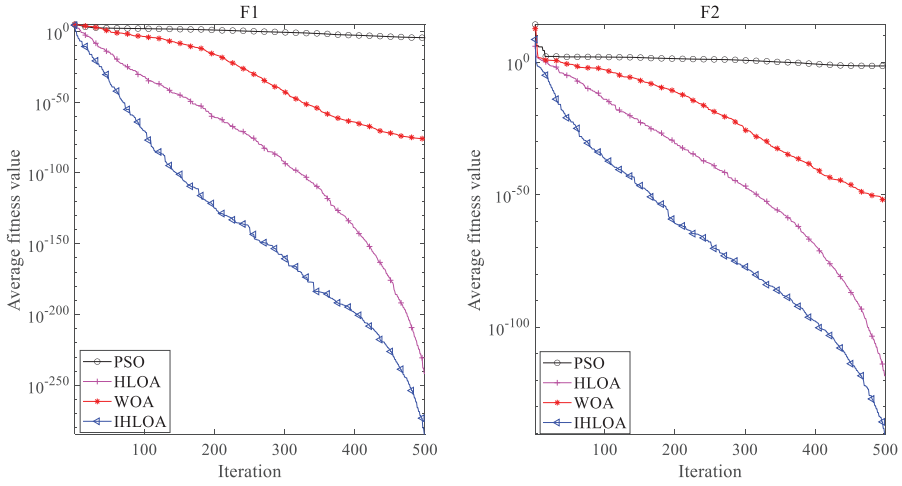

Figure 2: (Continued)

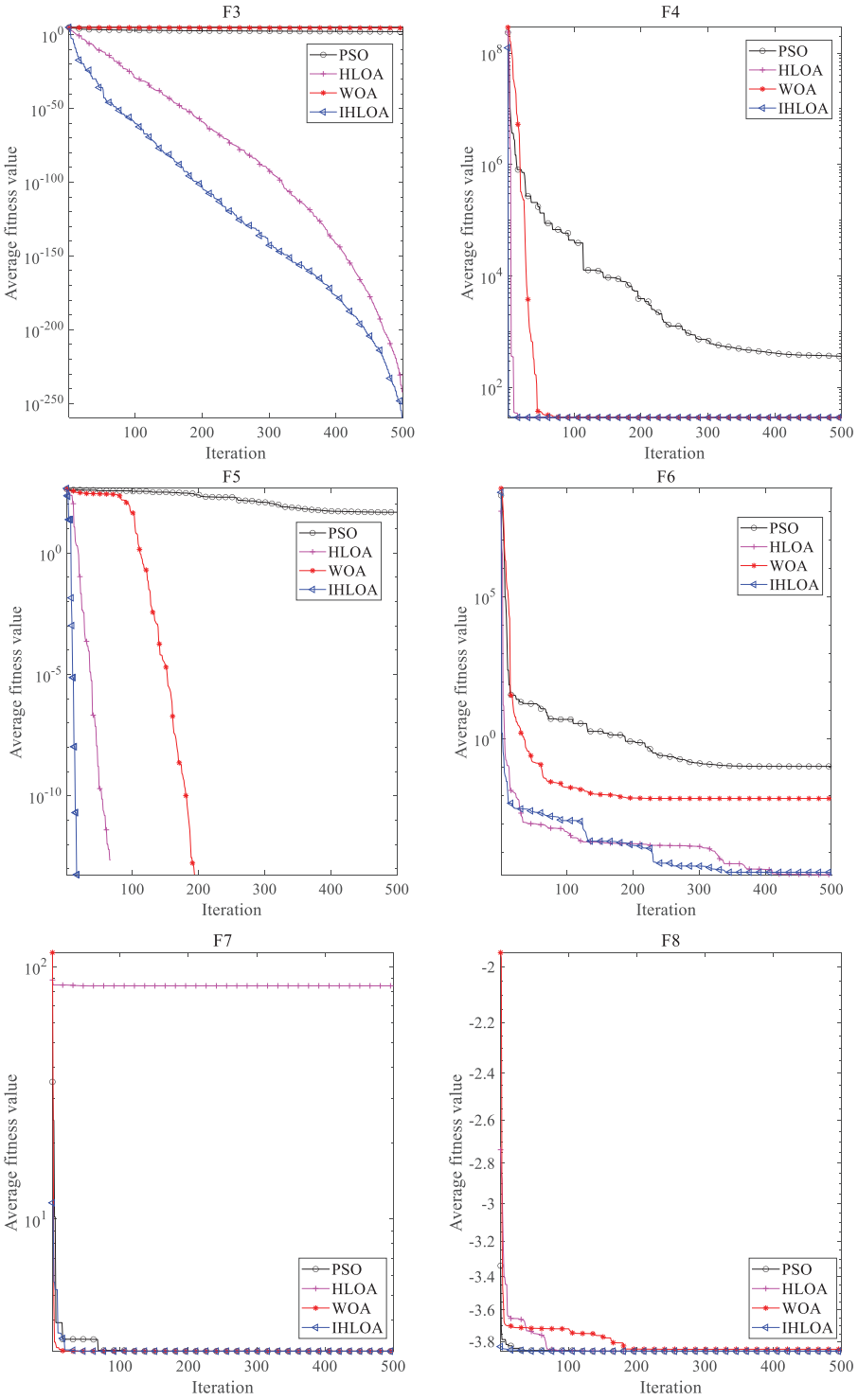

Figure 2: Convergence curves of different algorithms from F1 to F8

4 Experimental Validation

4.1 Case 1: Simulated Signal with Noise

In order to verify the denoising effect of IHLOA-VMD-wavelet thresholding secondary denoising method, the simulated signal is used, as follows:

$$\begin{cases} x1 = 0.25 \times cos(0.875 \times 50\pi t) \\ x2 = 0.3 \times sin(2\pi \times 50t) \times (1 + 1.5 \times sin(0.5\pi \times 40t)) \\ x3 = 0.15 \times exp(-15 \times t) \times sin(200\pi t) \end{cases} \tag{4}$$

$$x = x1 + x2 + x3 + nt$$

Among them, *nt* is random Gaussian white noise with a standard deviation of 0.2 added; The sampling frequency is 4000 Hz, and the time-domain waveform of the simulated signal with added noise is shown in the figure.

From Fig. 3, it is evident that the denoising method combining VMD and wavelet thresholding closely matches the original signal plot, indicating that a significant amount of noise has been eliminated. However, when using only wavelet denoising, the time-domain plot still contains residual noise.

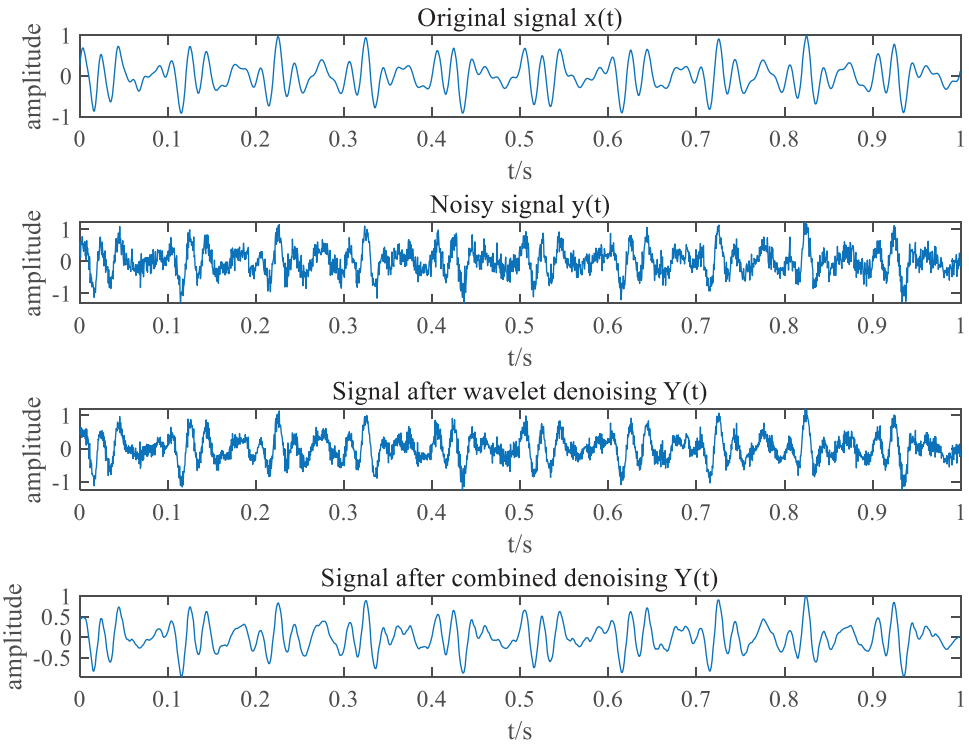

Figure 3: Time-domain diagram of simulated signal before and after denoising

To further verify the denoising effects, the following methods were applied to process the signal: VMD denoising, wavelet thresholding denoising, EMD denoising, CEEMDAN-wavelet thresholding denoising, and IHLOA-VMD-wavelet thresholding Combined denoising. The root mean squared error (RMSE) and signal-to-noise ratio (SNR) for each of the five denoising methods were calculated using the respective formulas.

Table 1 shows that the method proposed in this paper achieves the highest SNR and the smallest RMSE. A higher SNR indicates that more noise has been removed, resulting in a better denoising effect. The mean squared error measures the difference between the original signal and the denoised signal; a smaller mean squared error indicates that the denoised signal is closer to the original signal. Therefore, it can be concluded that the proposed method demonstrates superior denoising performance, making it both more effective and efficient.

Table 1: Mean square error and signal-to-noise ratio of different denoising methods

Method	SNR	RMSE
IHLOA+VMD+Wavelet Thresholding	17.7776	0.0447
CEEMDAN+Wavelet Thresholding	16.8475	0.0516
VMD	5.4762	0.3340
EMD	4.3262	0.4286
Wavelet	7.8876	0.1573

4.2 Case 2: Experimental Verification of Helical Gears

The gear data is sourced from the open-source dataset provided by Zamanian et al. [27–29]. Fig. 4 shows the gearbox test bench, which is designed to simulate and collect vibration signals from gears with different fault types, providing a solid foundation for subsequent model validation and performance evaluation. In the experiment, vibration signals were collected under a 20 Hz load. The fault signal for this gear has a sampling frequency of 10 kHz, a gear tooth count of $w = 15$, a shaft rotation frequency of 23.67 Hz and a gear mesh frequency of 365 Hz. The dataset includes three categories: normal, chipped tooth, and three worn teeth. In this study, a helical gear with chipped tooth is selected.

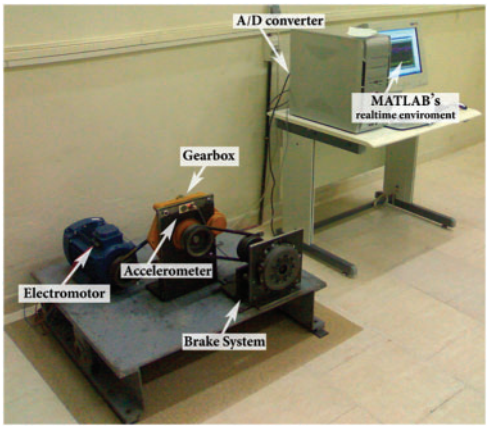

Figure 4: Gearbox test stand

The WOA, HLOA, and IHLOA algorithms were employed to search for the optimal parameters of VMD, with the minimum envelope entropy serving as the fitness function. Fig. 5 illustrates the variation of the function values. From the figure, it can be observed that IHLOA-VMD converges to the optimal solution within the third iteration. Compared to the WOA and HLOA algorithms, IHLOA shows superior search capability, faster convergence, and can efficiently identify the optimal VMD parameters. It has been proven

that the improved HLOA effectively avoids getting trapped in local optima, thereby enhancing the algorithm's overall performance.

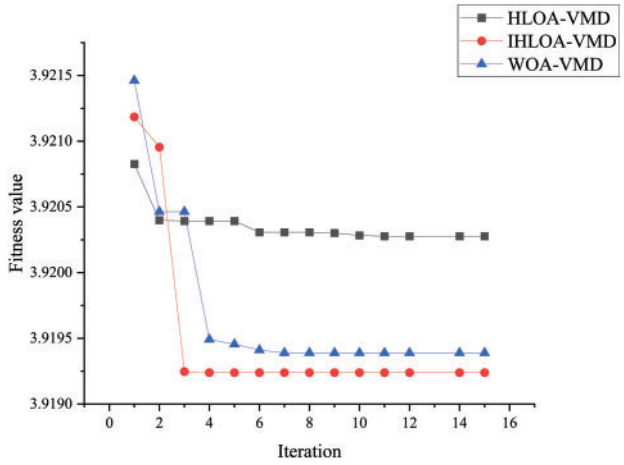

Figure 5: Variation of fitness function values for the fault signal of a helical gear with missing teeth

To verify the effectiveness of the proposed method, the correlation coefficient-variance of the six IMFs components decomposed by IHLOA-VMD were calculated, and the results are shown in Fig. 6. When the correlation coefficient-variance is very low, the explanatory power of the overall data is limited, and it may predominantly represent noise, failing to reflect the essential characteristics of the signal. Therefore, the components are classified into low-noise and high-noise components based on the correlation coefficient-variance. The low-noise component refers to the relatively pure part of the signal with minimal noise or interference, which closely resembles the original signal. In contrast, the high-noise component contains significant noise and interference, leading to poor performance after VMD processing. Due to the substantial impact of noise, the quality of this part of the signal is compromised. Since the high-noise component still contains useful information, wavelet thresholding is applied for secondary denoising to mitigate its influence.

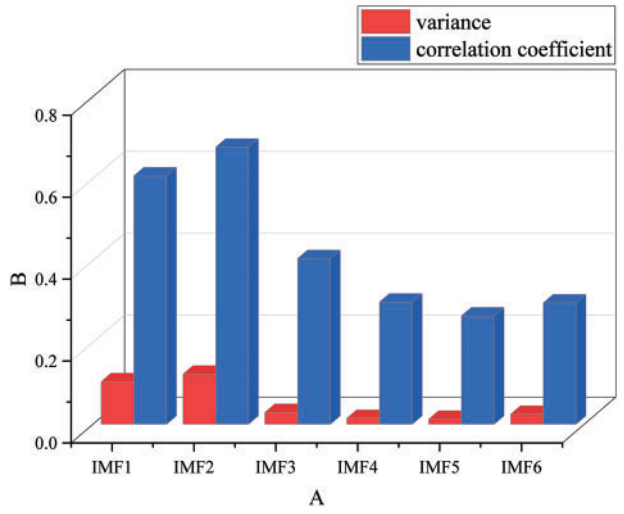

Figure 6: Correlation coefficients of various IMF vectors

By selecting IMF components with relatively low correlation coefficient-variance as high-noise components, high-variance modes typically represent the effective parts of the signal. In contrast, low-variance modes often contain noise or irrelevant information. Variance analysis helps in understanding the distribution of signal components and facilitates the separation of noisy signals from effective ones for reconstruction. Wavelet thresholding is then applied for secondary denoising, after which the denoised IMF components are reconstructed from the low-noise signal to produce the final denoised signal.

Since noise-free signals are unattainable, using SNR and root mean square error RMSE as evaluation indicators poses challenges. Therefore, Root of Variance Ratio (RVR) is introduced as a smoothness indicator, primarily used to assess the smoothness of the denoised signal. The closer its value is to 0, the better the smoothness, indicating more effective denoising. The Signal Energy Ratio (SER) is employed to measure the change in signal energy before and after denoising. A higher SER value generally reflects better preservation of the signal's main energy and effective suppression of noise components. Additionally, the Noise Mode (NM) index is used to evaluate changes in signal energy; a larger NM value indicates better preservation of the signal's effective components during the denoising process.

Table 2 shows a performance comparison of different methods based on three indicators: RVR, SER, and NM. The method proposed in this paper demonstrates significant advantages in overall performance: the RVR is 0.5966, which, although not the lowest, strikes a good balance; the SER is 0.90425, second only to VMD, and the NM is as high as 0.861, indicating a favorable balance between accuracy and denoising effect. In contrast, while VMD performs well on SER, its NM value is the lowest at only 0.0297, suggesting insufficient stability and overall performance. Therefore, the method proposed in this paper offers better noise reduction and broader applicability.

Table 2: RVR, SER and NM of different denoising methods

Method	RVR	SER	NM
IHLOA+VMD+WT	0.5966	0.90425	0.861
CEEMDAN+WT	0.3808	0.5949	0.7610
IHLOA+VMD+LMS	0.5602	1.2733	0.36672
VMD	0.6599	0.96339	0.0297
IHLOA+VMD+Kalman Fillter	0.0030	0.050102	0.9274

4.3 Case 3: Experimental Verification of Bevel Gear

To further validate the noise reduction method proposed in this paper for practical applications, using the gear dataset provided by HUST [30]. This dataset provides useful resources for research in gear fault diagnosis. Specifically, Fig. 7 illustrates the gearbox test bench at HUST. The design of this test bench allows for the simulation of various types of gear faults and the collection of their vibration signals, providing a solid foundation for subsequent experimental validation.

The sampling frequency of the experiment is 25.6 kHz, with two types of fault data for missing tooth and broken tooth. The spindle rotation frequency is 20 Hz, and the calculated gear meshing frequency is 360 Hz. Gaussian white noise of 1 dB is added to the signal.

When analyzing the IMF components processed by IHLOA-VMD, the correlation coefficient-variance of each component was first calculated, and the results were summarized in Fig. 8. IMF components with lower correlation coefficient-variance values were selected and reconstructed to form a new signal. Wavelet thresholding was then applied to this new signal, and the processed components were combined with

those having higher correlation coefficient-variance values for final signal reconstruction, resulting in the denoised signal.

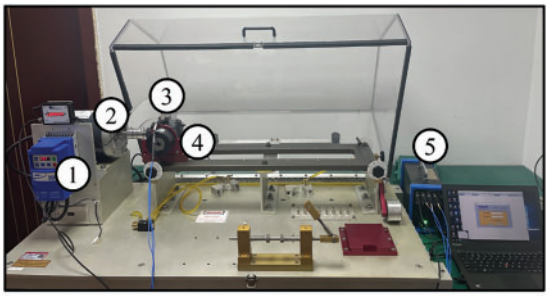

1: Speed control, 2:Motor, 3: Acceleration sensor, 4: gearbox, 5: Data acquisition board

Figure 7: Gearbox test bench at HUST

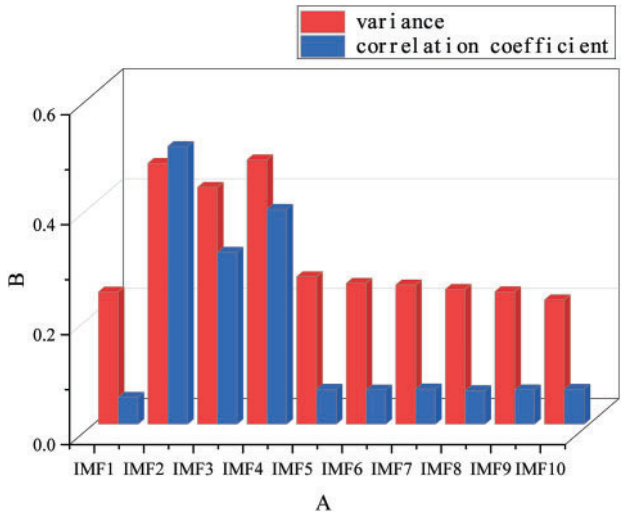

Figure 8: Correlation coefficients of various IMF vectors

Subsequently, the method proposed in this paper demonstrates strong performance by comparing the performance of different methods based on these evaluation indicators, particularly the data presented in the Table 3. Its RVR is only 0.0036, which is close to the minimum value, indicating extremely low deviation in signal recovery. The SER is 0.90285, the second-highest value, reflecting a good signal-to-noise ratio. Additionally, the NM value is 0.6644, balancing both stability and denoising effectiveness. In contrast, although VMD achieved the highest SER value of 1.1884, its RVR and NM performance were poor, indicating a lack of overall balance. Therefore, the method proposed in this paper offers comprehensive advantages across multiple indicators, with significant improvements in noise suppression and signal preservation.

To verify the universality of this method under different fault conditions, the signal of a broken tooth gear was used, and experimental verification was conducted following the same methodology. The PSO, WOA, HLOA, and IHLOA algorithms were employed to search for the optimal parameters of VMD, using the minimum envelope entropy as the fitness function. The function values are shown in the Fig. 9. It can

be observed from the figure that IHLOA-VMD finds the optimal solution the fastest. Compared to WOA, HLOA, and PSO algorithms, it exhibits stronger search capability and faster convergence speed and can efficiently identify the optimal parameters of VMD.

Table 3: RVR, SER and NM of different denoising methods

Method	RVR	SER	NM
IHLOA+VMD+WT	0.0036	0.90285	0.6644
CEEMDAN+WT	0.0083	0.63748	0.8024
IHLOA+VMD+LMS	0.0002	0.54409	0.5777
VMD	0.0040	1.1884	0.6163
IHLOA+VMD+Kalman Fillter	0	0.14071	0.8545

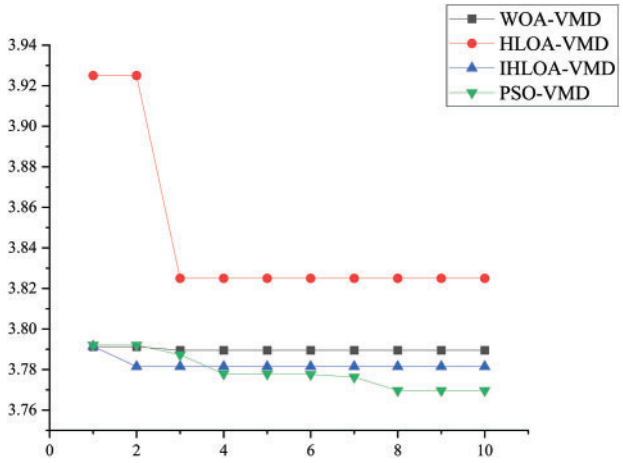

Figure 9: Changes in the fitness function value of the fault signal of a broken gear

The de-noised broken tooth signal obtained using the method proposed in this paper was compared with the de-noising effects of other methods. Verification was conducted using the three aforementioned indicators, and the results are shown in the Fig. 10: the symbol A represents IHLOA+VMD+Wavelet Threshold, the symbol B represents IHLOA+VMD+LMS, the symbol C represents IHLOA+VMD+Kalman Filter, and the symbol D represents CEEMDAN+Wavelet Threshold. Fig. 10 shows that the proposed method in this paper demonstrates superior performance in signal processing and noise reduction. In particular, it exhibits significant advantages regarding SER and NM, making it highly suitable for complex signal decomposition and noise suppression tasks.

Through the experimental comparisons presented above, although the method proposed in this paper may take slightly longer than the individual VMD and wavelet thresholding methods, the processing time is mainly influenced by the operating conditions, the number of iterations, and the population size of the optimization algorithm. However, the proposed method significantly enhances noise reduction and signal reconstruction performance through a multi-step process, demonstrating superior processing effects. In real-time condition monitoring of equipment, processing time is certainly important, but diagnostic accuracy and reliability are equally crucial. Considering both time efficiency and performance superiority, the method proposed in this paper, under multiple evaluation criteria, is more suitable for application in real-time

monitoring systems for equipment, providing effective fault detection and early early fault prediction while ensuring high-quality processing.

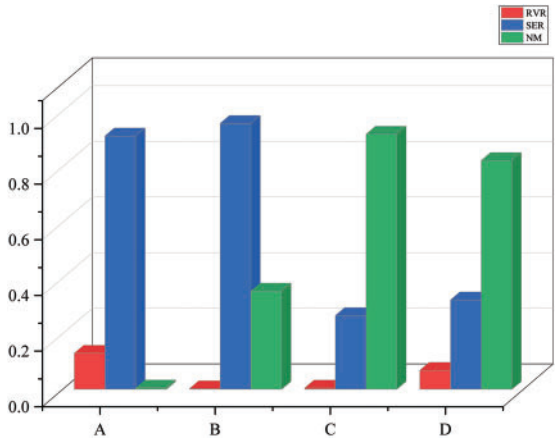

Figure 10: RVR, SER and NM of different denoising methods

The envelope spectrum of the original signal for the tooth breakage fault with 1 dB noise and the envelope spectrum after de-noising using IHLOA+VMD+Wavelet Threshold are shown in the Fig. 11 for comparison. Observing the de-noised envelope spectrum, it is evident that the meshing fault frequency is clearly visible after de-noising, and the sideband frequency features can be extracted. The spectral lines distributed uniformly on both sides of the harmonic frequencies are relatively lower. Therefore, the method proposed in this paper can effectively extract fault frequencies under noisy conditions, suppress the impact of noise on the signal, and demonstrate a certain degree of robustness against noise.

To validate the effectiveness of the proposed method, this paper compares the envelope spectra generated by the IHLOA-FMD method and the Multivariate Singular Spectrum Analysis (MSSA) method. From the results, it can be observed that the MSSA method's envelope spectrum still exhibits relatively high spectral lines on both sides, indicating the presence of noticeable residual noise. Additionally, the overall amplitude of the envelope is lower than that achieved by the proposed method, reflecting its limited ability to extract signal features effectively. In contrast, the IHLOA-FMD method's envelope spectrum shows more disorganized spectral line distributions on both sides, suggesting weaker noise suppression and insufficient de-noising performance. A comprehensive analysis demonstrates that the proposed method outperforms both in terms of de-noising effectiveness and signal feature extraction. It particularly shows strong robustness against noise interference, further validating the effectiveness and practical value of the proposed approach.

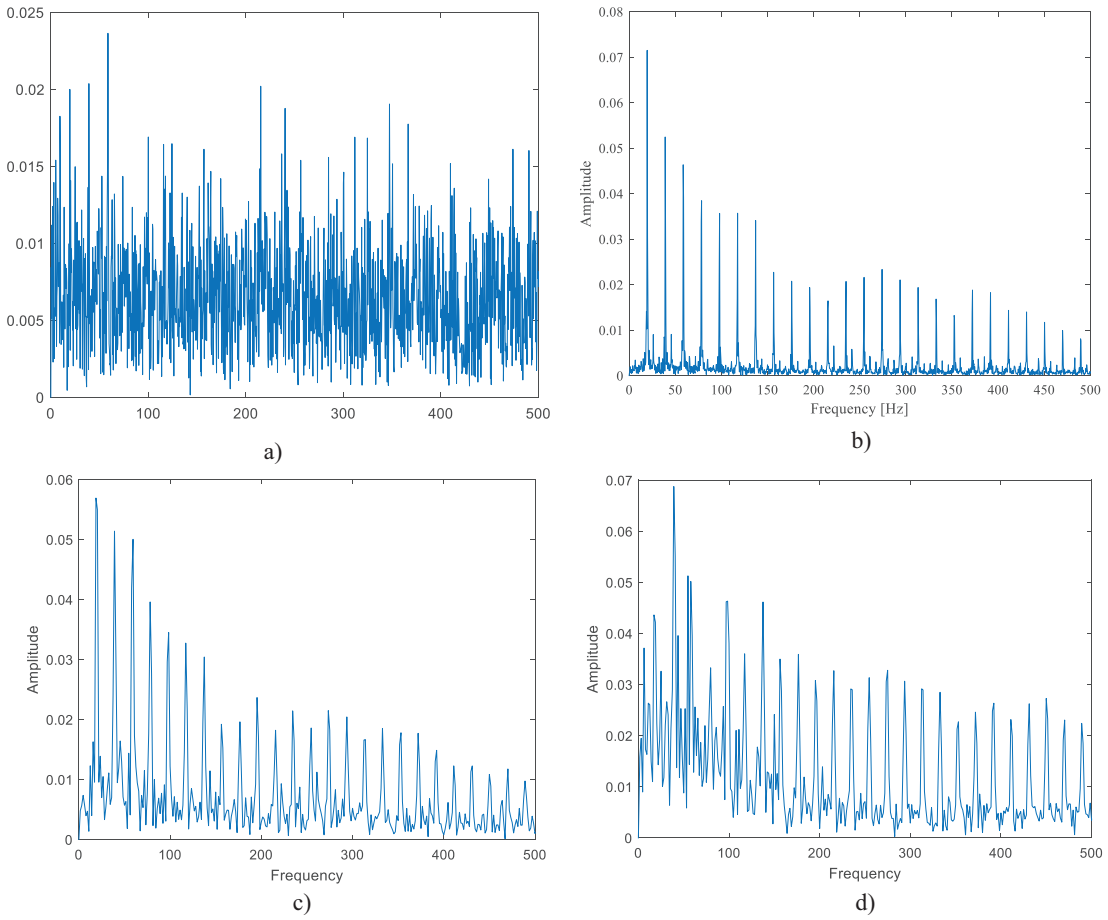

Figure 11: Envelope spectrum (a) Original signal with 1 dB noise (b) Envelope spectrum of the proposed method (c) Envelope spectrum of MSSA method (d) Envelope spectrum of IHLOA-FMD method

5 Conclusion

The IHLOA is proposed to optimize the VMD parameters and wavelet thresholding for combined denoising to reduce the noise of the acquisition signals from mechanical transmission systems. The main conclusions are as follows:

(1) To enhance the optimization efficiency of the HLOA algorithm and avoid local optima, an inertia weight parameter is incorporated into the random walk strategy. A comparison among HLOA, PSO, WOA, and IHLOA is conducted using eight standard benchmark functions. The results indicate that IHLOA significantly improves global and local search capabilities, overall convergence speed, and search accuracy.

(2) The IHLOA algorithm is employed to optimize the parameters of VMD, effectively mitigating mode aliasing and endpoint effects and achieving notable noise reduction. To retain useful information within high-noise components, wavelet thresholding is applied as a secondary denoising step. Simulation results validate the method's effectiveness, achieving a Signal-to-Noise Ratio (SNR) of 17.7776 and a Root Mean Square Error (RMSE) of 0.0447. Compared to other methods, this method achieves a higher SNR and a lower RMSE.

(3) Through the validation of signals related to gear tooth breakage and tooth loss, the results demonstrate that the proposed method can be effectively applied to other gear faults. By comparing the three

indicators—RVR, SER, and NM—it has been verified that the method excels in noise reduction, successfully minimizing noise interference in the signals. The experimental results fully prove the effectiveness and advantages of the method in signal denoising. Furthermore, by comparing the denoised signal waveforms of this method with those of IHLOA-FMD and Multivariate Singular Spectrum Analysis (MSSA), it is shown that the proposed method exhibits strong robustness in the presence of noise interference, thereby validating its effectiveness.

In short, the proposed IHLOA-VMD-wavelet thresholding method provides a robust solution for noise suppression in vibration signals and ensures accurate feature extraction. These capabilities are essential for ensuring the safety and reliability of mechanical systems in prognostic and health management.

Acknowledgement: None.

Funding Statement: The research was supported by Central Guidance on Local Science and Technology Development Fund of Hebei Province (Grant No. 226Z1906G), funded by Science Research Project of Hebei Education Department (CXY2024038), funded by Basic Research Project of Shijiazhuang University in Hebei Province (241791157A), National Natural Science Foundation of China (52206224).

Author Contributions: The authors confirm their contributions to the paper as follows: study conception and design: Guangfei Jia; data collection: Jinqiu Yang; analysis and interpretation of results: Guangfei Jia, Hanwen Liang; draft manuscript preparation: Jinqiu Yang. All authors reviewed the results and approved the final version of the manuscript.

Availability of Data and Materials: The authors confirm that the data supporting the findings of this study are available within the article.

Ethics Approval: Not applicable.

Conflicts of Interest: The authors declare no conflicts of interest to report regarding the present study.

Nomenclature

SNR	Signal-to-Noise Ratio
RMSE	Root Mean Square Error
EMD	Empirical Mode Decomposition
EEMD	Ensemble Empirical Mode Decomposition
CEEMD	Complementary Ensemble Empirical Mode Decomposition
CEEMDAN	Complementary Ensemble Empirical Mode Decomposition with Adaptive Noise
VMD	Variational Mode Decomposition
FMD	Feature Mode Decomposition
MSSA	Multichannel Singular Spectrum Analysis
PSO	Particle Swarm Optimization
WOA	Whale Optimization Algorithm
HLOA	Horned Lizard Optimization Algorithm
IHLOA	Improve Horned Lizard Optimization Algorithm
IMF	Intrinsic Mode Function
SER	Signal Energy Ratio
NM	Noise Modulus
WT	Wavelet Thresholding
RVR	Root of Variance Ratio
GMF	Gear Mesh Frequency
EWT	Empirical Wavelet Transform

References

1. Hu Y, Guo R, Wang H, Zhao R, Ning R, Huang Z, et al. Gear-fault monitoring and digital twin demonstration of aircraft engine based on piezoelectric vibration sensor for engine health management. Nano Energy. 2025;133:110448. doi:10.1016/j.nanoen.2024.110448.
2. Zhang L, He X, Chen J, Liu J. Fault diagnoses of a nonlinear cracked rotor-bearing system based on vibration energy space and incremental learning approach. J Sound Vib. 2025;600:118785. doi:10.1016/j.jsv.2024.118785.
3. Jia GF, Guo FW, Wu Z, Cui CX, Yang JJ. A noise reduction method for multiple signals combining computed order tracking based on chirplet path pursuit and distributed compressed sensing. Struct Durab Health Monit. 2023;17(5):383–405. doi:10.32604/sdhm.2023.026885.
4. Cheng J, Yang Y, Hu NQ, Cheng Z, Cheng JS. A noise reduction method based on adaptive weighted symplectic geometry decomposition and its application in early gear fault diagnosis. Mech Syst Signal Process. 2021;149(15):107351. doi:10.1016/j.ymssp.2020.107351.
5. Zhang Z, Liu X, Shu R, Xie F, Wang F, Liu Z, et al. A novel noise reduction method for space-borne full waveforms based on empirical mode decomposition. Optik. 2020;202:163581. doi:10.1016/j.ijleo.2019.163581.
6. Wang J, Du G, Zhu Z, Shen C, He Q. Fault diagnosis of rotating machines based on the EMD manifold. Mech Syst Signal Process. 2020;135(1):106443. doi:10.1016/j.ymssp.2019.106443.
7. Mao B, Bu Z, Xu B, Gong H, Li Y, Wang H, et al. Denoising method based on VMD-PCC in φ-OTDR system. Opt Fiber Technol. 2022;74(3):103081. doi:10.1016/j.yofte.2022.103081.
8. Li Z, Xiao J, Ding X, Wang L, Yang Y, Zhang W, et al. A new raw signal fusion method using reweighted VMD for early crack fault diagnosis at spline tooth of clutch friction disc. Measurement. 2023;220:113414.
9. Toffghi Niaki S, Alavi H, Ohadi A. Incipient fault detection of helical gearbox based on variational mode decomposition and time synchronous averaging. Struct Health Monit. 2023;22(2):1494–512. doi:10.1177/14759217221108489.
10. Matania O, Klein R, Bortman J. Transfer across different machines by transfer function estimation. Front Arttf Intell. 2022;5:811073. doi:10.3389/frai.2022.811073.
11. Wang W, Wong AK. Autoregressive model-based gear fault diagnosis. J Vib Acoust. 2002;124(2):172–9. doi:10.1115/1.1456905.
12. Wang WJ, McFadden PD. Decomposition of gear motion signals and its application to gearbox diagnostics. J Vib Acoust. 1995;117:363–9. doi:10.1115/1.2874462.
13. Huang NE, Shen Z, Long SR, Wu MC, Shih HH, Zheng Q, et al. The empirical mode decomposition and the Hilbert spectrum for nonlinear and non-stationary time series analysis. Proc Royal Soc London Ser A: Math Phys Eng Sci. 1998;454(1971):903–95. doi:10.1098/rspa.1998.0193.
14. Wu Z, Huang NE. Ensemble empirical mode decomposition: a noise-assisted data analysis method. Adv Adaptive Data Anal. 2009;1(1):1–41. doi:10.1142/S1793536909000047.
15. Chen C, Luo Y, Liu J, Yi Y, Zeng W, Wang S, et al. Joint sound denoising with EEMD and improved wavelet threshold for real-time drilling lithology identification. Measurement. 2024;238(1):115363. doi:10.1016/j.measurement.2024.115363.
16. Yeh JR, Shieh JS, Huang NE. Complementary ensemble empirical mode decomposition: a novel noise enhanced data analysis method. Adv Adapt Data Anal. 2010;2(2):135–56. doi:10.1142/S1793536910000422.
17. María ET, Marcelo AC, Gastón S, Flandrin P. A complete ensemble empirical mode decomposition with adaptive noise. In: 2011 IEEE International Conference on Acoustics, Speech and Signal Processing (ICASSP). 2011 May 22–27; Prague, Czech Republic. doi:10.1109/ICASSP.2011.5947265.
18. Gilles J. Empirical wavelet transform. Signal Process. 2013;61(16):3999–4010.
19. Li Z, Chen J, Zi Y, Pan J. Independence-oriented VMD to identify fault feature for wheel set bearing fault diagnosis of highspeed locomotive. Mech Syst Signal Process. 2017;85(11):512–29. doi:10.1016/j.ymssp.2016.08.042.
20. Chen HH. A vibration signal processing method based on SE-PSO-VMD for ultrasonic machining. Syst Soft Comput. 2024;6(14):20081. doi:10.1016/j.sasc.2024.200081.
21. Dragomiretskiy K, Zosso D. Variational mode decomposition. IEEE Trans Signal Process. 2013;62(3):531–44. doi:10.1109/TSP.2013.2288675.

22. Jiang H, Lu H, Zhou J, Liu M. Fault diagnosis of rolling bearings in VMD and GWOELM. J Phys: Conf Ser. 2023;2496(1):012013. doi:10.1088/1742-6596/2496/1/012013.
23. Lin Y, Xiao M, Liu H, Li Z, Zhou S, Xu X, et al. Gear fault diagnosis based on CS-improved variational mode decomposition and probabilistic neural network. Measurement. 2022;192(19):110913. doi:10.1016/j.measurement.2022.110913.
24. Zhang X, Miao Q, Zhang H, Wang L. A parameter-adaptive VMD method based on grasshopper optimization algorithm to analyze vibration signals from rotating machinery. Mech Syst Signal Process. 2018;108(12):58–72. doi:10.1016/j.ymssp.2017.11.029.
25. Ding J, Huang L, Xiao D, Li X. GMPSO-VMD algorithm and its application to rolling bearing fault feature extraction. Sensors. 2020;20(7):1946. doi:10.3390/s20071946.
26. Peraza-Vázquez H, Peña-Delgado A, Merino-Treviño M, Morales-Cepeda AB, Sinha N. A novel metaheuristic inspired by horned lizard defense tactics. Artif Intell Rev. 2024;57(3):59. doi:10.1007/s10462-023-10653-7.
27. Zamanian AH. Experimental dataset for gear fault diagnosis. 2014. doi:10.13140/RG.2.2.28152.44802/2.
28. Zamanian AH, Ohadi A. Gear fault diagnosis based on Gaussian correlation of vibrations signals and wavelet coefficients. Applied Soft Comput. 2011;11(8):4807–19. doi:10.1016/j.asoc.2011.06.020.
29. Zamanian AH, Ohadi A. Gearbox fault detection through PSO exact wavelet analysis and SVM classifier. In: 18th Annual International Conference on Mechanical Engineering—ISME; May 2010; Tehran, Iran: Sharif University of Technology. doi:10.13140/RG.2.1.4983.3442.
30. Zhao C, Zio E, Shen WM. Domain generalization for cross-domain fault diagnosis: an application-oriented perspective and a benchmark study. Reliab Eng Syst Saf. 2024;245:109964. doi:10.1016/j.ress.2024.109964.